Study of resonances in the complex charge plane

2004 J. Phys. A: Math. Gen. 37 5863

(http://iopscience.iop.org/0305-4470/37/22/011)

INSTITUTE OF PHYSICS PUBLISHING JOURNAL OF PHYSICS A: MATHEMATICAL AND GENERAL

J. Phys. A: Math. Gen. **37** (2004) 5863–5871 PII: S0305-4470(04)78055-5

Study of resonances in the complex charge plane

A D Alhaidari

Physics Department, King Fahd University of Petroleum & Minerals, Dhahran 31261, Saudi Arabia

E-mail: haidari@mailaps.org

Received 17 March 2004
Published 18 May 2004
Online at stacks.iop.org/JPhysA/37/5863
DOI: 10.1088/0305-4470/37/22/011

Abstract

Potential resonances are usually investigated either directly in the complex energy plane or indirectly in the complex angular momentum plane. Another formulation complementing these two approaches is presented in this work. It is an indirect algebraic method that studies resonance in a complex charge plane (Z-plane). The complex scaling (rotation) method is employed in the development of this formulation. A finite L^2 basis is used in the numerical implementation of the method.

PACS numbers: 03.65.Nk, 03.65.Ca, 02.30.Tb, 03.65.Fd

1. Introduction

Obtaining energy resonances is of prime significance in the study of potential scattering. Several techniques have been developed by many researchers over the years for locating resonances (position and width) of various interaction models[1]. The objective of most of these studies is to increase the accuracy of the values obtained, and to improve the computational efficiency in locating resonances. All of these investigations are performed in one of two modes: either directly in the complex energy plane or indirectly in the complex angular momentum plane. In the former setting the energy spectrum of the Hamiltonian (poles of Green's function) generally consists of three parts: (1) a discrete set of real points on the negative energy axis corresponding to the bound states, (2) the real positive energy line which corresponds to the continuum scattering states and (3) another discrete set of points in the

[1] The volume of publications on this topic is overwhelming. Interested readers are advised to consult any of the searchable databases to run refined searches, with as many relevant keywords, to obtain manageable output on a specific interest. Books and articles cited in this work and references therein are examples of such publications with broad coverage. However, a good start could be the book by Kukulin *et al* [1].

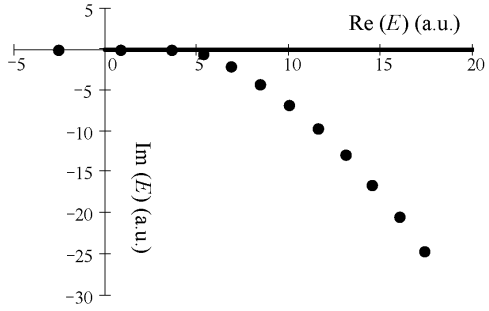

Figure 1. The poles (dots) and discontinuity (line) of the p-wave Green function in the complex energy plane for the system whose potential is given by equation (1.1). One bound state and 11 resonances (two being sharp) are shown.

lower half of the complex energy plane corresponding to resonance states. These are bound-like states that are unstable, decaying with a rate that increases with the (negative) value of the imaginary part of the resonance energy. That is, sharp or 'shallow' resonances (those located below and close to the real energy axis) decay much slower than broad or 'deep' resonances that are located below, but far from, the real energy axis. Figure 1 shows such a typical structure, which is associated with the potential

$$V(r) = 5\mathrm{e}^{-(r-\frac{7}{2})^2/4} - 8\mathrm{e}^{-r^2/5}. \tag{1.1}$$

On the other hand, resonances could also be studied in the complex angular momentum plane by locating the Regge poles [2] for a given energy and investigating their trajectories as the (complex) energy is varied. Resonance energies are those that correspond to points on the trajectories that cross the real angular momentum axis at non-negative integers ($\ell = 0, 1, 2, \ldots$). Figure 2(a) shows an example of trajectories associated with the potential (1.1) for a given range of energies with a fixed negative imaginary part, and displays the lowest five trajectories. It indicates the presence of an $\ell = 3$ resonance. Figure 2(b) shows trajectories for the same system, but in which the energies are real. These do not cross the real ℓ-line. Nonetheless, they could still be used to extract resonance information.

The basic principle underlying the various numerical methods used for the study of resonance, which are implemented within one of these two formulations, is that the position of a resonance is stable against variation in all computational parameters. In this work the same principle will be used to introduce a third formulation that complements the two approaches that were explained briefly above. The analysis of resonance in this formulation is performed in a complex charge plane. We employ the complex scaling (rotation) method [3] in the development of this formalism. A simple potential example will be given to demonstrate the utility and accuracy of this method. The results obtained from such an analysis will be compared with those found elsewhere in the literature. Additionally, new resonances are calculated, with some being so broad that they are beyond the range of applicability of some present techniques.

2. Complex scaling in the charge plane

By complex scaling or complex rotation we mean the transformation of the radial coordinate r as shown by

$$r \to r\,\mathrm{e}^{\mathrm{i}\theta} \tag{2.1}$$

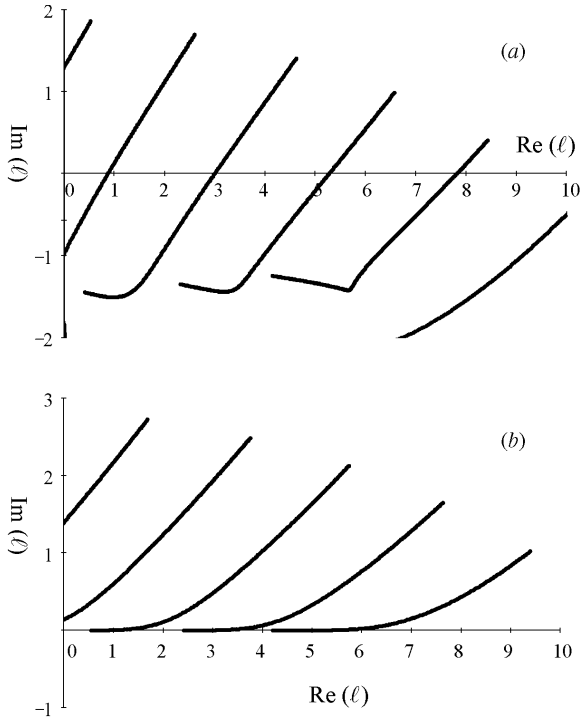

Figure 2. (*a*) The trajectory of Regge poles in the complex ℓ-plane for the system whose potential is given by equation (1.1). Along these trajectories the real part of the energy varies smoothly from 3.0 to 10.0 au, while the imaginary part is fixed at -2.0 au. The graph indicates the presence of a resonance where the trajectory crosses the real line at $\ell = 3$. Our calculation gives the following value for this resonance: $E = 7.091\,723\,04 - \mathrm{i}2.001\,734\,29$ au. (*b*) Regge trajectories plot for the same system as used for (*a*), with the exception that the imaginary part of the energy vanishes. These trajectories start on the real axis and bend upwards as the energy increases.

where θ is a real angular parameter. The Green function (resolvent operator) is formally defined as $G^\theta \equiv (H^\theta - E)^{-1}$, where E is the complex energy and H^θ is the complex-rotated full Hamiltonian of the system. The effect of this transformation on the pole structure of the Green function in the complex energy plane consists of the following: (1) the discrete bound state spectrum that lies on the negative energy axis remains unchanged; (2) the branch cut (the discontinuity) along the real positive energy axis rotates clockwise by the angle 2θ and (3) resonances in the lower half of the complex energy plane located in the sector bound by the new rotated cut line and the positive energy axis get exposed and become isolated. However, due to the finite size of the basis used in performing the calculation, the matrix representation of the Hamiltonian is finite resulting in a discrete spectrum. Consequently, the rotated cut line is replaced by a string of interleaved poles and zeros of the finite Green function, which tries to mimic the cut structure. This method will now be developed to make it suitable for implementation in the complex charge plane.

In the atomic units $\hbar = m = 1$, the one-particle wave equation for a spherically symmetric potential $V(r)$ in the presence of the Coulomb field reads

$$(H - E)\chi = \left[-\frac{1}{2}\frac{\mathrm{d}^2}{\mathrm{d}r^2} + \frac{\ell(\ell+1)}{2r^2} + \frac{Z}{r} + V(r) - E\right]\chi = 0 \tag{2.2}$$

where ℓ is the orbital angular momentum and Z is the electric charge in units of e. $\chi(r)$ is the wavefunction that is parametrized by ℓ, Z, E and the potential parameters. Equation (2.2) could be rewritten as $(\hat{H} - Z)\hat{\chi} = 0$, where

$$\hat{H} = \frac{r}{2}\frac{\mathrm{d}^2}{\mathrm{d}r^2} - \frac{\ell(\ell+1)}{2r} + rE - rV(r) \equiv \hat{H}_0 + \hat{V} \tag{2.3}$$

and $\hat{V} \equiv -rV(r)$. The continuum could be discretized by taking $\hat{\chi}$ as an element in an L^2 space with a complete basis set $\{\phi_n\}$. The integration measure in this space is $\mathrm{d}r/r$. We parametrize the basis by a length scale parameter λ as $\{\phi_n(\lambda r)\}$. The following realization of the basis functions is compatible with the domain of the operator $\hat{H}$ and satisfies the boundary conditions (at $r = 0$ and $r \to \infty$)

$$\phi_n(\lambda r) = A_n x^{\alpha}\, \mathrm{e}^{-x/2} L_n^{\nu}(x) \tag{2.4}$$

where $x = \lambda r$, $\alpha > 0$, $\nu > -1$ and $n = 0, 1, 2, \ldots$. $L_n^{\nu}(x)$ is the Laguerre polynomial of order n and A_n is the normalization constant $\sqrt{\Gamma(n+1)/\Gamma(n+\nu+1)}$. The choice $2\alpha = \nu + 1$ makes the basis set $\{\phi_n\}$ orthonormal. The matrix representation of the 'reference' operator $\hat{H}_0$ in this basis is written as

$$(\hat{H}_0)_{nm} = \langle \phi_n(x)| \frac{\lambda}{2} x \frac{\mathrm{d}^2}{\mathrm{d}x^2} - \ell(\ell+1)\frac{\lambda}{2x} + \frac{E}{\lambda} x \,|\phi_m(x)\rangle\,. \tag{2.5}$$

Consequently, the action of the transformation (2.1) on $\hat{H}_0$ is equivalent to

$$\lambda \to \lambda\, \mathrm{e}^{-\mathrm{i}\theta}. \tag{2.6}$$

In the manipulation of (2.5) we use the differential equation, differential formulae and three-term recurrence relation of the Laguerre polynomials [4]. As a result, we obtain the following elements of the matrix representation of the reference operator:

$$\begin{aligned}(\hat{H}_0)_{nm} = {} & \lambda\left(\frac{E}{\lambda^2} - \frac{1}{8}\right)(2n+\nu+1)\delta_{n,m} - \lambda\left(\frac{E}{\lambda^2} + \frac{1}{8}\right)\sqrt{n(n+\nu)}\,\delta_{n,m+1} \\ & - \lambda\left(\frac{E}{\lambda^2} + \frac{1}{8}\right)\sqrt{(n+1)(n+\nu+1)}\,\delta_{n,m-1} + \frac{\lambda}{8}[\nu^2 - (2\ell+1)^2](x^{-1})_{nm}\end{aligned} \tag{2.7}$$

where the symmetric matrix $(x^{-1})_{nm} = \frac{1}{\nu}(A_{n_>}/A_{n_<})$ and $n_>$ ($n_<$) is the larger (smaller) of n and m. To simplify this representation we take $\nu = 2\ell + 1$, which results in a tridiagonal matrix representation for $\hat{H}_0$. Now, the only remaining quantity that is needed to perform the calculation is the matrix elements of the 'potential' term $\hat{V}$ as defined in equation (2.3). This is obtained by evaluating the integral

$$\begin{aligned}\hat{V}_{nm} &= \int_0^{\infty} \phi_n(\lambda r)[-rV(r)]\phi_m(\lambda r)\frac{\mathrm{d}r}{r} \\ &= \frac{-1}{\lambda} A_n A_m \int_0^{\infty} x^{\nu}\, \mathrm{e}^{-x} L_n^{\nu}(x) L_m^{\nu}(x)[xV(x/\lambda)]\,\mathrm{d}x.\end{aligned} \tag{2.8}$$

The evaluation of such an integral is almost always done numerically. We use the Gauss quadrature approximation [5], which gives

$$\hat{V}_{nm} \cong \frac{-1}{\lambda} \sum_{k=0}^{N-1} \Lambda_{nk}\Lambda_{mk}[\mu_k V(\mu_k/\lambda)] \tag{2.9}$$

for an adequately large integer N. μ_k and $\{\Lambda_{nk}\}_{n=0}^{N-1}$ are the respective N eigenvalues and eigenvectors of the $N \times N$ tridiagonal symmetric J matrix whose elements are

$$J_{n,n} = 2n + \nu + 1 \qquad J_{n,n+1} = -\sqrt{(n+1)(n+\nu+1)}. \tag{2.10}$$

These findings will be used in the following section to locate and analyse the resonance structure for the potential $V(r) + Z/r$ in the complex Z-plane. An example will be given to illustrate the utility and demonstrate the accuracy of the proposed method.

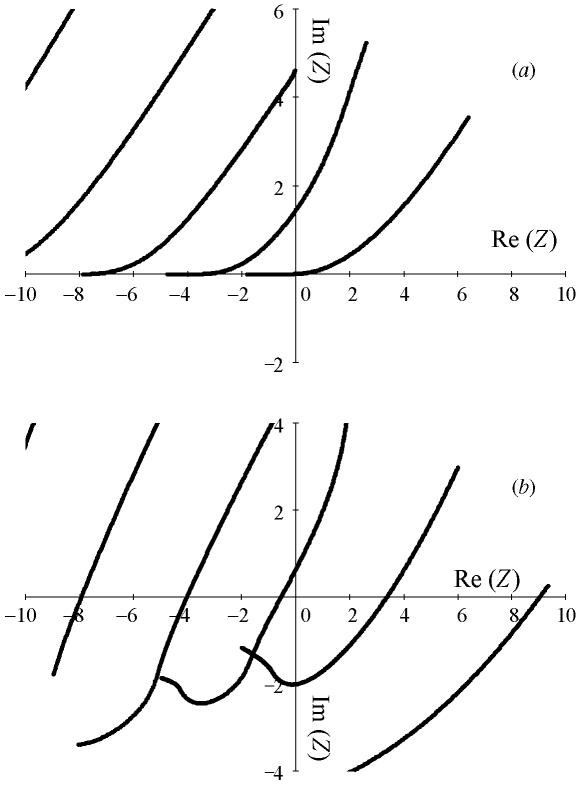

Figure 3. (*a*) The trajectory of the poles of the s-wave Green function $\hat{G}^{\theta}(Z)$ in the complex Z-plane for the system whose potential is $7.5r^2\,\mathrm{e}^{-r} + Z/r$. Along these trajectories the energy is real, and varies smoothly from 0.0 to 10.0 au. They start on the real Z-axis for lower energies and bend upwards as the energy increases. (*b*) Same as (*a*), with the exception that the energy is now complex with a negative imaginary part that is kept constant at −3.0 au. The crossings at, or near, $Z = -8$, -4 and 9 signify resonances that are calculated as 1.287 274 955 − i2.971 759 279, 3.125 581 370 − i3.023 378 045, and 9.733 679 948 − i2.988 524 088 au, respectively.

3. Studying resonance in the complex Z-plane

The system described by equation (2.2) may be studied by investigating an equivalent system as described by the equation $(\hat{H} - Z)\hat{\chi} = 0$. However, this equivalence is only an approximation that improves with an increase in the size of the basis, N. Our investigation of the latter system is made by using the method of complex rotation which, as explained previously, is implemented by applying the transformation $\lambda \to \lambda\,\mathrm{e}^{-\mathrm{i}\theta}$ on the matrix representations (2.7) and (2.9). The resulting complex eigenvalues $\{Z_n\}_{n=0}^{N-1}$ of $\hat{H}^{\theta}$ are the poles of the finite Green's function $\hat{G}^{\theta} = \left(\hat{H}_0^{\theta} + \hat{V}^{\theta} - Z\right)^{-1}$. The subset of these poles that are stable (in the complex Z-plane) against variation in the parameters λ and θ are the poles that are physically significant. However, θ must always be larger than the minimum angle needed to expose the poles of interest. The branch cut of Green's function $\hat{G}(Z)$ is located on the negative Z-axis. Complex scaling rotates this cut clockwise through the angle θ and exposes the relevant poles. This behaviour may be understood by comparing it with the corresponding one in the complex energy plane, and noting that (i) the relative sign of Z to that of E in the Hamiltonian (2.2) is negative, and (ii) the length dimensions of E and Z are the same as those of λ^2 and λ,

Table 1. Resonance energies ($E = \mathcal{E}_r - i\Gamma/2$) for the potential $7.5r^2\,e^{-r} + Z/r$. Our results are compared with those found in the cited references. Stability of our calculation is based on a substantial range of variation in λ ($\sim$5 to 100 au) and θ ($\sim$0.5 to 1.0 radians). The accuracy is relative to a basis dimension of $N = 200$.

Z	$\mathcal{E}_r$ (au)	Γ (au)	Reference
0	3.426 39	0.025 549	[6]
	3.425 7	0.025 6	[7]
	3.426	0.025 6	[8]
	3.426	0.025 8	[9]
	3.426 390 331	0.025 548 962	[10]
	3.426 390 310	0.025 548 961	This work
0	4.834 806 841	2.235 753 338	[10]
	4.834 806 841	2.235 753 338	This work
0	5.277 279 780	6.778 106 356	[10]
	5.277 279 864	6.778 106 591	This work
-1	1.780 5	9.58×10^{-5}	[9]
	1.780 524 536	9.5719×10^{-5}	[10]
	1.780 524 536	$9.571\,94 \times 10^{-5}$	This work
-1	4.101 494 946	1.157 254 428	[10]
	4.101 494 946	1.157 254 428	This work
-1	4.663 461 099	5.366 401 539	[10]
	4.663 461 097	5.366 401 540	This work

respectively. As we vary the energy (generally, complex), the poles of $\hat{G}^\theta$ move along trajectories in the complex Z-plane. The points where the *stable* trajectories cross the real Z-axis correspond to resonances. For elementary charged particles scattering, the relevant crossings are those at $Z = 0, \pm1, \pm2, \ldots$.

The union of all of the sets of eigenvalues $\{Z_n(E)\}_{n=0}^{N-1}$ for a given range of (complex) values of E produces N trajectories in the Z-plane. The physically relevant ones are those which are stable against variation (around a plateau) in all computational parameters. However, it should be noted that the ordering of these eigenvalues by the index n is computation-dependent and is not necessarily the same for two different values of E. Consequently, one has to plot all of the eigenvalues for each E in the energy range to see the full picture. To illustrate these findings we consider, as an example, the potential function

$$V(r) = 7.5r^2\,e^{-r} \tag{3.1}$$

which has been studied frequently in the literature [6–10]. Figure 3(*a*) shows the lowest s-wave trajectories for real energies. They start on the real Z-axis for low energies and bend upwards as the energy increases. The same graph is repeated in figure 3(*b*), but now the energy has a non-vanishing imaginary part. It shows several crossings at, or near, $Z = -8$, -4 and 9, indicating resonance. In practice, we vary the imaginary part of E until it produces trajectory plots that have at least one branch crossing the real Z-axis at, or very close to, an integral value. Subsequently, we zoom in at one of the crossings by stretching the scale of the real Z-axis where we will find that the crossing is not quite at the integral value of Z. Thus, we need to fiddle with a higher significant digit in the imaginary part of the energy to bring the trajectory crossing back to the integral value. This process continues until we reach the limit of accuracy which is indicated by erratic behaviour of the trajectory points that can only be eliminated by an increase in the size of the space, N. On the other hand, the accuracy of the real part of the energy is improved by iteration of successive steps of (1) reducing the length of

Table 2. A more comprehensive list of resonances for the same potential as in table 1, and for several values of Z and ℓ.

	$\ell = 0$		$\ell = 1$		$\ell = 2$	
Z	$\mathcal{E}_r$ (au)	Γ (au)	$\mathcal{E}_r$ (au)	Γ (au)	$\mathcal{E}_r$ (au)	Γ (au)
0	5.064 929 608	11.952 069 576	5.427 742 2973	9.280 688 974	5.793 693 0648	6.660 951 732
	4.268 860 299	17.433 816 868	5.360 469 6511	4.394 482 330	5.502 943 9380	11.843 122 555
	2.947 781 6003	23.061 029 462	4.887 769 0564	14.623 615 321	5.491 345 3119	2.107 291 5737
	1.147 183 738	28.738 014 274	4.646 634 4207	0.650 589 0286	4.652 774 2298	17.324 910 417
	−1.096 688 979	34.402 043 587	3.801 798 4630	20.187 028 641	3.289 231 6413	22.949 471 910
	−3.754 144 12	40.009 014 99	2.218 906 3561	25.846 441 901	1.452 991 4754	28.624 988 427
	−6.800 304	45.526 31	0.178 577 3686	31.524 321 640	−0.821 534 539	34.290 493 164
	−10.21	50.93	−2.286 964 11	37.167 523 861	−3.505 402 56	39.902 0901
			−5.150 992	42.737 42	−6.5742	45.4265
			−8.39	48.20	−10.0	51
−1	4.561 151 055	10.413 396 043	4.932 942 955	8.233 838 942	5.300 613 4903	5.884 714 861
	3.849 197 760	15.816 567 000	4.750 053 489	3.505 579 849	5.088 641 4686	10.943 326 210
	2.593 348 5088	21.387 481 635	4.476 218 206	13.477 261 705	4.900 516 1468	1.567 507 0165
	0.844 647 138	27.021 909 107	3.848 001 6348	0.275 384 4592	4.300 179 8532	16.341 585 409
	−1.356 846 588	32.653 003 793	3.453 996 8253	18.968 736 871	2.986 244 924	21.903 035 992
	−3.978 854 424	38.234 130 33	1.921 603 5248	24.572 340 524	1.190 735 6869	27.527 998 140
	−6.9947	43.730 92	−0.077 733 2579	30.205 316 536	−1.049 790 7711	33.151 641 912
	−10.38	49.1	−2.509 315 965	35.811 697 83	−3.704 884 68	38.727 911 891
			−5.344 69	41.351 08	−6.749 011	44.222 22
			−8.56	46.8	−10.16	49.61
+1	5.867 437 031	8.158 768 524	5.940 903 6759	5.280 262 4063	6.269 729 8719	7.448 168 504
	5.569 681 242	3.422 105 119	5.902 424 814	10.320 417 212	6.057 188 1775	2.690 560 7459
	5.545 052 842	13.452 0219 82	5.371 865 4458	1.146 241 8923	5.905 180 463	12.745 6471 81
	4.666 831 409	19.017 323 601	5.284 083 4258	15.761 247 384	4.996 063 0849	18.307 602 572
	4.594 490 160	0.257 890 6726	4.137 209 0078	21.396 522 076	3.584 578 573	23.993 734 433
	3.282 757 1775	24.707 275 525	2.505 669 7545	27.112 401 950	1.708 693 6696	29.719 160 385
	1.432 515 0596	30.432 561 004	0.425 698 1801	32.836 153 732	−0.599 061 162	35.426 371 269
	−0.851 599 9765	36.134 066 609	−2.072 721 3505	38.517 201 91	−3.311 106 73	41.073 405 78
	−3.542 588 981	41.770 275 53	−4.964 49	44.118 55	−6.404 053	46.628 23
	−6.617 38	47.310 57	−8.2283	49.6	−9.86	52.07
	−10.056	52.73				

the trajectory to a minimum by refining the range of the real part of the energy that produced it and (2) zooming in vertically by stretching the scale of the imaginary Z-axis. A numerical algorithm using bisection or Newton–Raphson routines [11] could be developed to automate the search.

In our calculation, we start with a rough estimate of resonance values obtained by the complex rotation method [3] for the potential (3.1). The level of accuracy of the proposed formalism is then demonstrated by improving on these values for a given size of the basis. Table 1 compares values found in the literature to those obtained in this work. Other resonances are also obtained in table 2, some of which are very broad. Stability of these results against variation in λ and θ (for a basis size $N = 200$) is observed up to the tenth decimal place.

Nonetheless, the merit of the present approach is not in the accuracy of the results obtained, but rather in the global picture that it gives for the overall behaviour of resonance and its structure. For this it is endowed with formal and computational analogies to the Regge

poles and Regge trajectories in the complex ℓ-plane. Specifically, it has close similarities to the Regge–Sommerfeld–Watson method in dealing with poles and trajectories allowing for the use of all the analytic and numerical tools used in that theoretical scheme. In particular, the scattering matrix could be studied by the analysis of the poles and their trajectories in the complex Z-plane in much the same way as that involving the analysis of Regge poles and Regge trajectories in the complex ℓ-plane. However, one of its advantages is that it is an algebraic method, which may find wide acceptance among many researchers who prefer such an approach over analytic ones for the purpose of ease of numerical computations. Another advantage is that it gives in one comprehensive picture the overall behaviour of the scattering matrix for different values of the charge coupling Z. Needless to say, it is not an alternative to the methods that study resonances in the E- and ℓ-planes but, as previously stated, complementary to them. Moreover, since the orbital angular momentum is a fundamental physical quantity which is present in all spherically symmetric interactions, this gives the Regge theory wider range of applicability. It is only when charged particles are involved in the scattering that it makes the present approach more suited for these studies. Additionally, if only s-wave scattering is of prime interest then the present approach might take precedence.

The reference Hamiltonian H_0 which we have considered in this paper involves the Coulomb interaction Z/r. Consequently, without any further investigation this approach is suited only for applications of scattering processes involving charged particles. The scattering of neutral particles is obviously a special case. However, it is believed that this technique could also be extended to other classes of interactions. We are presently, investigating the class of exactly solvable potentials which includes, amongst others, the oscillator, Coulomb, Morse, Scarf, Pöschl–Teller. Preliminary encouraging results have already been obtained and our findings will be reported in the near future.

Acknowledgments

The author is grateful to H A Yamani and M S Abdelmonem for fruitful discussions that provided motivation for this work.

References

[1] Kukulin V I, Krasnopolsky V M and Horáček J 1988 *Theory of Resonances* (Dordrecht: Kluwer)
[2] De Alfaro V and Regge T 1965 *Potential Scattering* (Amsterdam: North-Holland)
Taylor J R 1972 *Scattering Theory* (New York: Wiley)
Sitenko A G 1991 *Scattering Theory* (Heidelberg: Springer)
[3] Aguilar J and Combes J M 1971 *Commun. Math. Phys.* **22** 269
Balslev E and Combes J M 1971 *Commun. Math. Phys.* **22** 280
Simon B 1972 *Commun. Math. Phys.* **27** 1
Cerjan C, Hedges R, Holt C, Reinhardt W P, Scheibner K and Wendoloski J J 1978 *Int. J. Quantum Chem.* **14** 393
Reinhardt W P 1982 *Ann. Rev. Phys. Chem.* **33** 223
Junker B R 1982 *Adv. At. Mol. Phys.* **18** 208
Ho Y K 1983 *Phys. Rep.* **99** 1
Maquet A, Chu Shih-I and Reinhardt W P 1983 *Phys. Rev.* A **27** 2946
[4] Magnus W, Oberhettinger F and Soni R P 1966 *Formulas and Theorems for the Special Functions of Mathematical Physics* (New York: Springer) pp 239–49
Abramowitz M and Stegun I A (ed) 1964 *Handbook of Mathematical Functions* (New York: Dover)
[5] See, for example, Appendix A in Alhaidari A D, Yamani H A and Abdelmonem M S 2001 *Phys. Rev.* A **63** 062708

[6] Isaacson A D, McCurdy C M and Miller W H 1978 *Chem. Phys.* **34** 311
[7] Maier C H, Cederbaum L S and Domcke W 1980 *J. Phys. B: At. Mol. Phys.* **13** L119
[8] Mandelshtam V A, Ravuri T R and Taylor H S 1993 *Phys. Rev. Lett.* **70** 1932
[9] Yamani H A and Abdelmonem M S 1995 *J. Phys. A: Math. Gen.* **28** 2709
[10] Sofianos S A and Rakityansky S A 1997 *J. Phys. A: Math. Gen.* **30** 3725
[11] Press W H, Flannery B P, Teukolsky S A and Vetterling W T 1986 *Numerical Recipes* (New York: Cambridge University Press)